

# Electrode/Electrolyte Interface Studies in Lithium Batteries Using NMR

by Nicolas Dupré, Marine Cuisinier, and Dominique Guyomard

Easy access to portable energy sources has become necessary for the last decades and rechargeable batteries are now omnipresent in everyday tools and devices thanks to their storage capacity and relatively low weight. More recently, the possible use of lithium-ion batteries in full electric and hybrid electric vehicles has attracted considerable attention. However, great challenges still remain in this area of research and the importance of interfaces has become especially obvious in the field of electrochemistry and its applications to energy storage devices.<sup>1,2</sup> The solid electrolyte interphase (SEI) between the negative electrode and the electrolyte of a Li-ion battery is known to factor into the overall battery behavior in terms of irreversible capacity loss, charge transfer kinetics, and storage properties.<sup>3-6</sup> More than ten years of research in this field have led to excellent control and optimization of the SEI layer on carbon electrodes. Surface formulation and/or coatings of the positive electrode have been shown more recently to influence the battery performance as well.<sup>7-11</sup> Interfacial reactions and the growth of a passivation layer at the electrode surface upon cycling have been also highlighted for different positive electrode materials and have been identified to be of paramount importance as they can lead to performance degradation of the battery upon aging and cycling.<sup>12,13</sup> The existence of surface reactions at the positive electrode/electrolyte interface has been clearly demonstrated but the experimental conditions of formation, growth and modification, as well as its subsequent influences on the electrochemical performance, remain unclear. The chemical, physical, and structural properties of the interfacial layer at the positive electrode in particular are still not well known, and thus this more recent research area is of great interest.<sup>14-18</sup>

This article gives an overview of the NMR approach developed to extract and interpret information on the electrode/electrolyte interphase in lithium battery materials to probe evolution of electrochemical behavior and/or failure mechanisms along electrochemical cycling of lithium batteries. Such approach focuses on *ex situ* analysis of electrode materials. Recent studies have shown that *in situ/operando* NMR signals can be obtained during electrochemical processes<sup>19-21</sup> but these works mainly focus on the interpretation of bulk electrochemical mechanisms and therefore, are not discussed in the present article.

First are summarized the results of works dealing with the extraction and interpretation, from NMR data, of chemical information based on the chemical shift of various nuclei, and of quantitative information based on the integrated intensities of NMR signals.

The theory required to interpret NMR spectra of paramagnetic samples and to extract information on the interaction of surface layers with the electrode material bulk is then briefly described in order to make it accessible to the non-NMR audience. An earlier review article gives a more comprehensive description of the chemical and physical information that can be extracted from the presence of unpaired localized electrons.<sup>22</sup> This second part is then followed by illustrative examples obtained from stored or cycled electrode materials.

## Use of NMR to Characterize Interface Species on Non-Paramagnetic Materials

Insofar NMR can be used to detect lithium, phosphorus, hydrogen, carbon, and fluorine among others, it appears as an appropriate method to study species present on surfaces of electrode materials, resulting from electrolyte decomposition. Among the numerous techniques to study the evolution of SEI on graphitic electrodes, Greenbaum *et al.*<sup>23</sup> used electrochemical impedance spectroscopy (EIS) and solid-state <sup>7</sup>Li NMR techniques to characterize the films formed on graphite anodes in low-temperature electrolytes with different mixtures of alkyl-carbonates and low-viscosity solvent additives such as aliphatic esters. A quantitative determination of SEI Li content was obtained by integrating the <sup>7</sup>Li NMR signals associated with Knight-shifted intercalated Li and unshifted Li species residing in the SEI. A compact, barrier-type, protective film is formed in alkyl-carbonate based solutions, whereas porous, and less protective films are formed with DME additives. The same group investigated the SEI on LiNi<sub>0.8</sub>Co<sub>0.2</sub>O<sub>2</sub><sup>24</sup> while Tucker *et al.*<sup>25</sup> showed the presence of Li-containing species on the particles surface of substituted LiMn<sub>2</sub>O<sub>4</sub> spinel-type materials upon moisture contamination using <sup>7</sup>Li MAS NMR. The positive electrode cycled at room temperature builds up an interphase displaying similar NMR spectra with respect to that of stored positive electrodes, although in lower amount. By comparing relative integrated intensities assigned to the SEI and to lithium ions inserted in the

cathode (in that case at 580 ppm), the SEI growth can be quantitatively monitored by NMR methods. More recently, <sup>7</sup>Li MAS NMR analyses of the charged silicon electrodes demonstrated that the major part of the lithium lost during the charge of batteries is not trapped in Li<sub>x</sub>Si alloys but instead at the surface of the Si particles, likely as a degradation product of the liquid electrolyte.<sup>26</sup> Based on the different shifts observed for Li<sub>x</sub>Si alloys,<sup>21</sup> it was demonstrated that the main cause of capacity fade of Si-based negative electrodes is the liquid electrolyte degradation in the case of nano-Si particles formulated with the carboxymethyl cellulose (CMC) binder. This degradation leads to the formation of a blocking layer on the active material, which further inhibits lithium diffusion through the electrode porosity.

Diamagnetic species containing Li, which NMR signals rise at approx. 0 ppm are frequently observed on numerous systems but not really investigated beyond a semi-quantitative analysis of the integrated intensity using <sup>7</sup>Li NMR due to the narrow chemical shift range,<sup>27</sup> typically between 2.8 ppm for Li<sub>2</sub>O and -1.1 ppm for LiCl (Fig.1). The discrimination between several diamagnetic lithiated species present at the same time in the interphase might prove difficult. The interest of employing <sup>19</sup>F or <sup>31</sup>P NMR resides in the much wider chemical shift that can be used to identify fluorine or phosphorus containing products (Fig. 2), ranging in <sup>19</sup>F NMR from -72.4 ppm for PF<sub>6</sub><sup>-</sup> to the products of its hydrolysis at -76.7 ppm (PO<sub>3</sub>F<sup>2-</sup>), -83.8 ppm (PO<sub>2</sub>F<sub>2</sub><sup>-</sup>), -153.7 (HF) and -204 ppm for LiF,<sup>28</sup> and ranging in <sup>31</sup>P NMR from -146 ppm for PF<sub>6</sub><sup>-</sup> to -10.1 ppm (PO<sub>3</sub>F<sup>2-</sup>), -21.6 ppm (PO<sub>2</sub>F<sub>2</sub><sup>-</sup>). It becomes then possible to detect typical LiPF<sub>6</sub> decomposition products already observed by other techniques.<sup>18, 29-32</sup>

First, <sup>19</sup>F NMR results drew attention to the presence of a fluorine-containing compound in the interphase, distinct from the background signal of the PVDF binder. The complementary use of <sup>7</sup>Li and <sup>19</sup>F NMR appeared indeed extremely useful to identify LiF as one of the decomposition products of LiPF<sub>6</sub> (usual salt of Li-ion battery electrolytes) despite LiF invisibility in the mid-IR (~700 to 1400 cm<sup>-1</sup>) range.<sup>33</sup> Its formation in the solid electrolyte interphase (SEI) at both graphite and LiCoO<sub>2</sub> electrodes in lithium-ion rechargeable batteries was monitored quantitatively.<sup>27</sup> This study allowed establishing correlations between the amount of LiF formed on the cathode with both the number of cycles and the Li loss percentage from

(continued on next page)

the cathode while no correlation was found for LiF vs. cycle number for the anode.

In addition to this wider detection range and in order to investigate the organic components of the SEI,  $^{13}\text{C}$  NMR provides a way to follow the decomposition reaction of organic carbonates yielding the organic part of the SEI as performed on the carbonaceous anodic electrode in C/LiCoO<sub>2</sub> batteries.<sup>34</sup> NMR signals assigned to lithium-based carbon derivatives showed that the Li-salt reacts with solvent, leading to accumulation of decomposition products on the electrode particles surface.<sup>35</sup> Furthermore, the use of  $^{13}\text{C}$  enriched ethylene-carbonate and diethyl-carbonate solvents allowed following the decomposition pathway, indicating the presence of carbonyl groups in SEI layer, demonstrating a nucleophilic attack mechanism on the carbonyl carbon by one or more radical, alkoxy, carbanion, or fluorine-containing ionic species formed from solvent and/or salt decomposition. These results suggest a new family of electrolyte breakdown products, predominantly consisting of binary, ternary, and/or quaternary ether-type compounds (i.e., orthocarbonates and orthoesters), as well as fluorine-containing alkoxy compounds.<sup>34</sup>

Most of these studies, done on diamagnetic materials, rely only on the interpretation of the chemical shift to determine the chemical nature of the species formed from electrolyte decomposition, and on the monitoring of the integrated intensity to follow the progress of that reaction. In the case of transition metal compounds, NMR detection is more complicated, especially due to fast relaxation time leading to broadening of the signal caused by the presence of paramagnetic centers. However the resulting NMR spectra contain valuable additional information on the interaction between surface species and active electrode material bulk.

### Use of NMR to Characterize Interface Species on Paramagnetic Materials

Magic angle spinning (MAS) NMR is generally used to characterize bulk materials. The Fermi contact interaction along with the electron-nucleus dipolar interactions and their respective effects on the  $^6\text{Li}$  NMR spectra have been widely discussed in the case of lithium ions present within the host matrix of the insertion material.<sup>22,36</sup> The corresponding mechanisms have also recently been investigated using theoretical calculations.<sup>37-39</sup> Like the Chemical Shift Anisotropy (CSA), the electron-nucleus dipolar interaction scales with the field. At high field, even

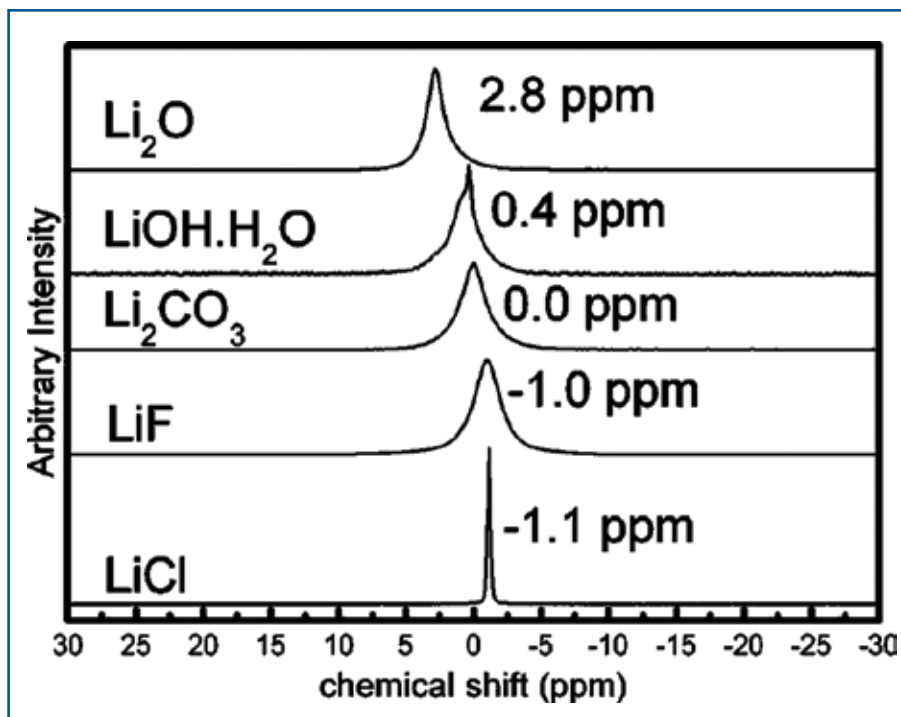


Fig. 1.  $^7\text{Li}$  spectra showing chemical shift for various inorganic compounds that may be present in a SEI layer. (Reprinted with permission from Ref. 27)

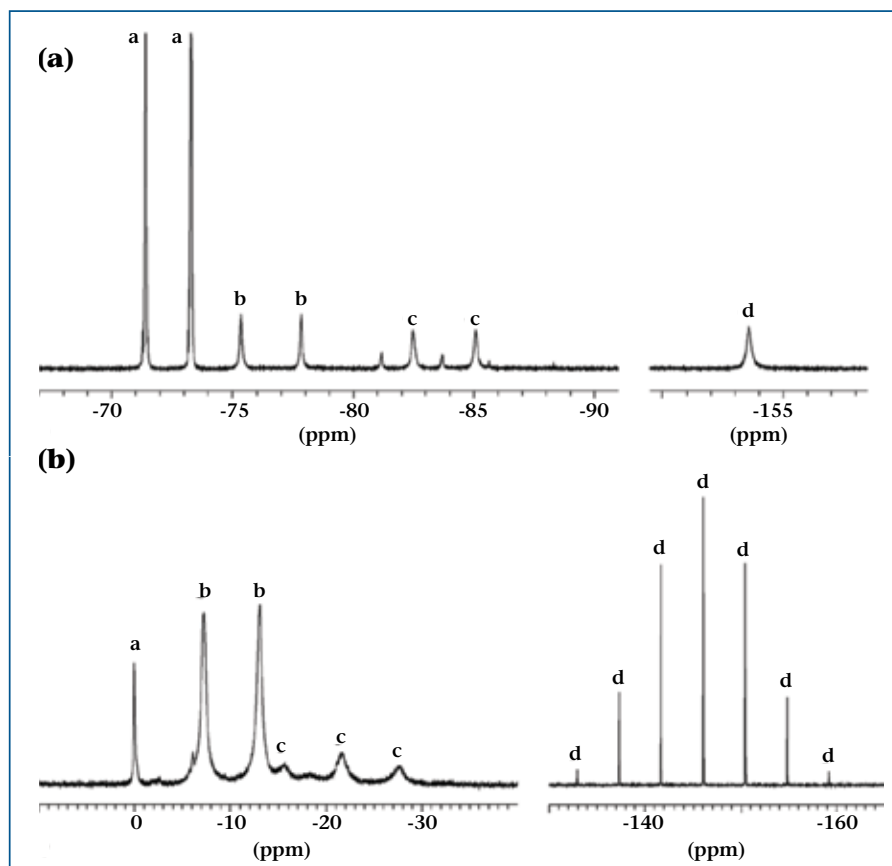


Fig. 2. Typical  $^{19}\text{F}$  and  $^{31}\text{P}$  NMR spectra of the  $\text{LiPF}_6$ -containing solutions and of the products of  $\text{LiPF}_6$  hydrolysis. (a) Signals a, b, c, and d are assigned to  $\text{PF}_6^-$ ,  $\text{PO}_3\text{F}^-$ ,  $\text{PO}_2\text{F}_2^-$ , and HF, respectively. (b) Signals a, b, c, and d belong to  $\text{H}_3\text{PO}_4$ ,  $\text{PO}_3\text{F}^-$ ,  $\text{PO}_2\text{F}_2^-$ , and  $\text{PF}_6^-$ , respectively. (Reprinted with permission from Ref. 28, license number 2713681279312)

a fast spinning frequency does not allow averaging the interaction. Therefore, a very broad and unresolved signal is typically seen for lithium ions within the structure of the host matrix (Fig. 3). This signal is usually shifted due to the strong Fermi-contact interaction and according to the distribution of transition metals carrying localized unpaired electrons.<sup>22,40,41</sup> Much narrower signals, superimposed to the bulk signal, were observed by Tucker *et al.*<sup>25</sup> and Ménétrier *et al.*<sup>42</sup> between 0 and 1 ppm. This narrow signal can be assigned to Li present outside the active material in a surface layer. No departure of the isotropic resonance from the diamagnetic chemical shift range is observed in this case, indicating that the detected surface layer, composed of diamagnetic lithium-containing species, is not chemically bonded with the bulk active material, and therefore it is presumed to be predominantly physisorbed. NMR is a quantitative technique and thus all lithium nuclei in the sample are detected using <sup>6,7</sup>Li NMR. However, since the quantity of lithium in surface species is much smaller than the quantity of lithium within the bulk of host material, it becomes difficult to obtain accurate information on “surface” lithium from the complete spectrum.

Exerting through space, with a  $1/r^3$  dependence on the distance, this strong dipolar interaction is a very efficient relaxation mechanism for the NMR magnetization. Based on the extremely fast relaxation observed for lithium in the bulk material compared to that of lithium in diamagnetic secondary phase(s), a single pulse with a long pre-acquisition delay suppresses the broad signal from bulk lithium making the signal assigned to surface lithium much more pronounced and easier to analyze. The weaker interaction felt by Li in the interphase allows resolving the NMR signal into spinning sidebands even at high field. Since the size of the dipolar coupling depends on the gyromagnetic ratio,  $g_N$ , larger dipolar couplings are seen for nuclei with larger values of  $g_N$ . Thus, <sup>7</sup>Li with its much larger gyromagnetic ratio than <sup>6</sup>Li ( $g_{7Li}/g_{6Li} = 2.6$ ) results in MAS spectra with much larger spinning sideband manifolds and easier to interpret.

Using first this method in a study of the so-called interphase layer present at the surface of  $\text{Li}(\text{Ni}_{1-y-z}\text{CoAl}_z)\text{O}_2$ , Ménétrier *et al.*<sup>42</sup> mentioned the influence on the lineshape of MAS NMR spectra of the strong through-space dipolar interaction between the electron spins of the paramagnetic material and lithium nuclei in the surface layer,

resulting in broadening of the sidebands manifold over a wide frequency range. In that case, this discrimination method in <sup>7</sup>Li NMR, along with <sup>1</sup>H NMR was used to understand the evolution of the nature of the surface layer upon hydration of the material. In particular, results indicated the presence of protons intercalated in the material, which amount increases upon hydration, thus releasing lithium ions that form the growing layer. More recently, this method proved appropriate and straightforward to probe the surface of electrode materials as <sup>7</sup>Li and <sup>19</sup>F MAS NMR analyses revealed unambiguously the presence of fluorine as a LiF “coating” on the surface of the  $\text{Li}(\text{Ni}_{0.425}\text{Mn}_{0.425}\text{Co}_{0.15})\text{O}_2$  particles, rejecting the formation of fluorine-substituted  $\text{Li}_x(\text{Ni}_{0.425}\text{Mn}_{0.425}\text{Co}_{0.15/0.9}\text{O}_{1-x}\text{F}_{0.2})$  materials<sup>43,44</sup> claimed to be obtained by several authors based on changes in cell parameters observed using X-ray diffraction.<sup>45-47</sup>

Following this precursor work, a <sup>7</sup>Li MAS NMR study of physisorbed surface layers on  $\text{LiNi}_{1/2}\text{Mn}_{1/2}\text{O}_2$  has been performed<sup>42,48</sup> on a series of samples obtained by mixing the material with lithium carbonate or from contact of the material with ambient atmosphere, as well as with electrolyte. The progressive narrowing of the sidebands manifold of MAS NMR spectra reflects the decreasing intimacy or increasing distance of surface lithium with bulk material (Fig. 4) and therefore can yield extremely useful information complementary to the chemical information obtained from XPS or FTIR.

However, when considering such a signal, it appears that it cannot be considered as a single lithium site but it is rather a superposition of resonances corresponding to a distribution of lithium ions. They are ranging from locations close to the surface of the bulk material, on the inside of a secondary phase dispersed on the bulk material grains, to locations on the outside of this surface phase. Then the observed signal should evolve according to two parameters: the thickness of the surface phase and its intimacy with the bulk.

Spin-lattice ( $T_1$ ) relaxation time measurements can be used as a probe of surface layers, allowing the discrimination of interphases from different origins. The  $b$  and  $T_1$  values obtained using a stretched exponential<sup>48</sup> can describe the growth of a layer on the surface of the grains of active material and an evolution of the intimacy between the surface layer and the active material. For instance,  $T_1$  increases and  $b$  decreases as the thickness increases, reflecting the decreasing influence of the paramagnetic phase on the relaxation time with the distance and the subsequent wider distribution of  $T_1$  values, respectively. This method

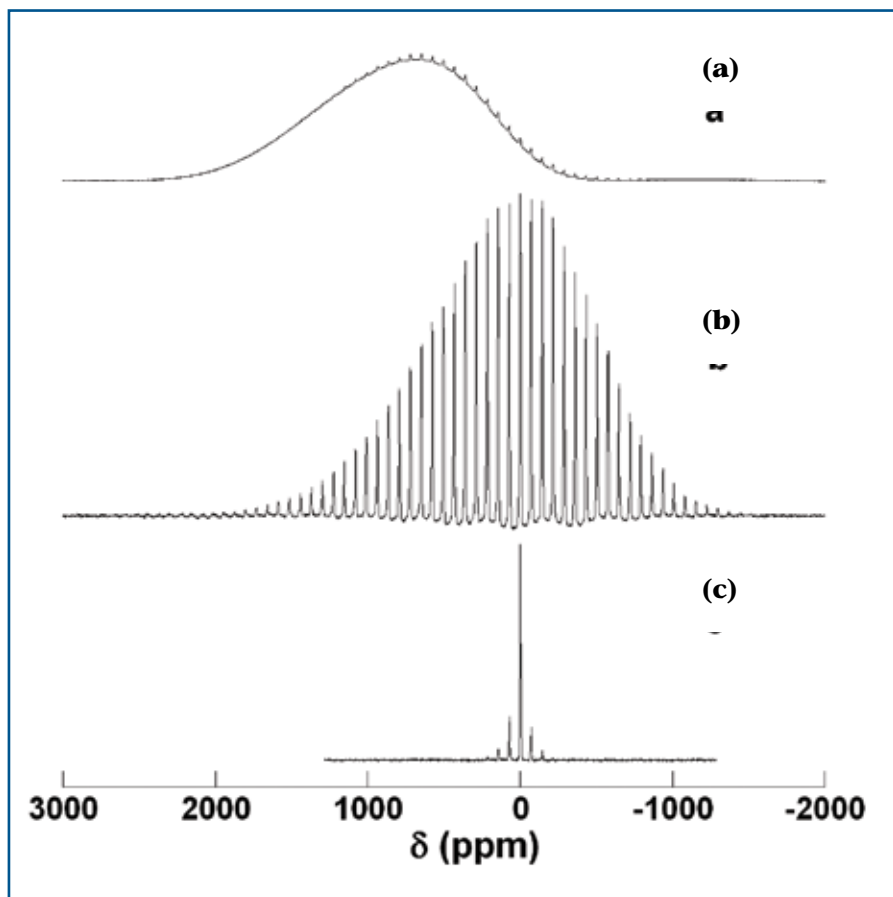


**Fig. 3.** <sup>7</sup>Li MAS NMR spectra for  $\text{LiNi}_{1/2}\text{Mn}_{1/2}\text{O}_2$  stored in ambient atmosphere for two months acquired (a) with a Hahn-echo pulse sequence, (b) with a single pulse sequence, and (c)  $\text{Li}_2\text{CO}_3$  as a reference. (Reprinted with permission from Ref. 48)

(continued on next page)

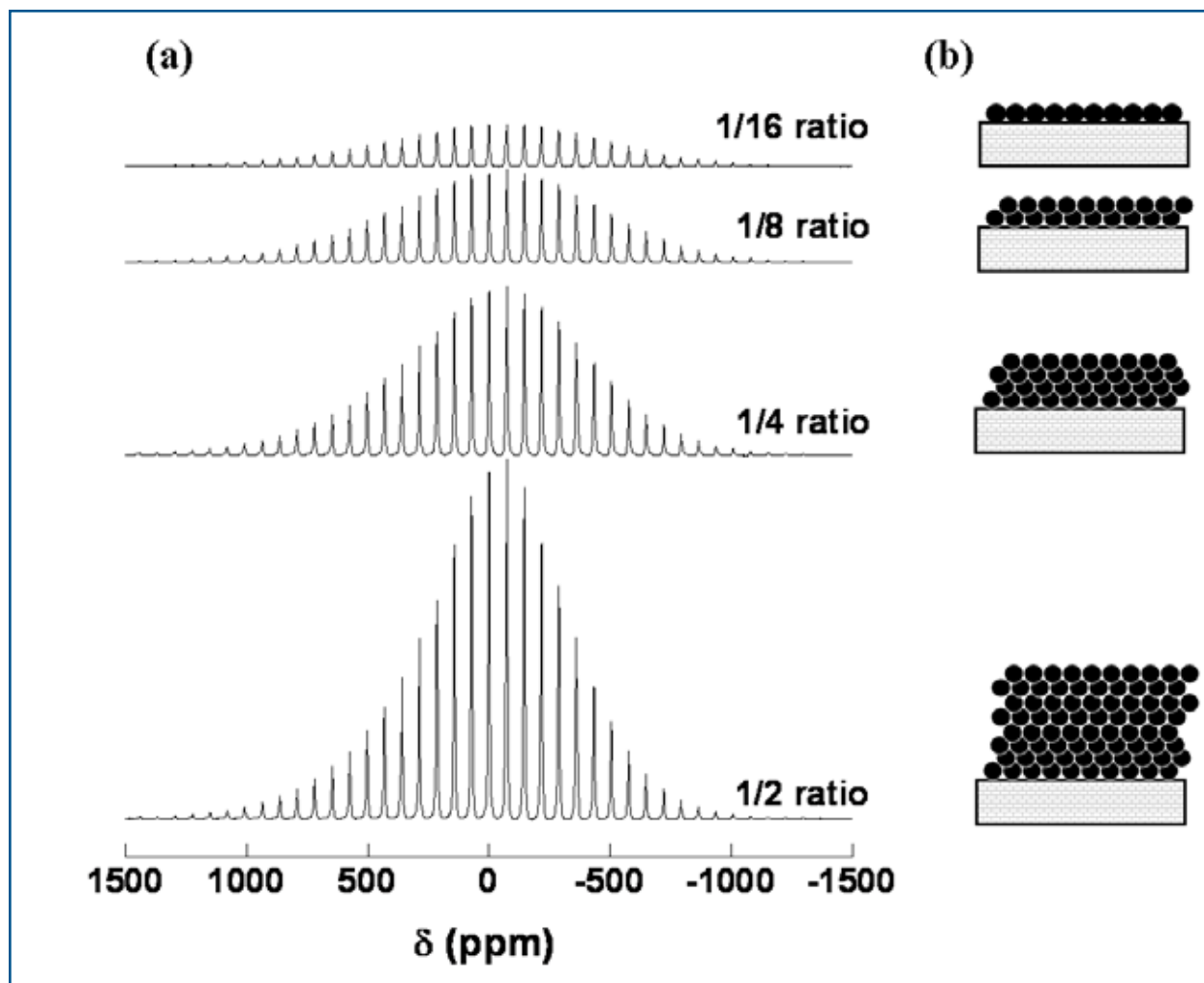


**Fig. 4.** (a)  ${}^7\text{Li}$  MAS NMR spectra for  $\text{LiNi}_{1/2}\text{Mn}_{1/2}\text{O}_2$  ball-milled with various  $\text{Li}_2\text{CO}_3/\text{LiNi}_{1/2}\text{Mn}_{1/2}\text{O}_2$  weight ratios. The ratios are indicated in the figure. (b) schemes showing the amount of lithium species on the surface of active material. The white rectangles represent an idealized section of the surface of one particle of active material and the black disks represent particles or aggregates of diamagnetic lithium-containing species. (Reproduced by permission of The Royal Society of Chemistry)

of characterization using NMR measurements seems promising but has been applied so far only on samples obtained by mixing paramagnetic electrode material and known amount of diamagnetic lithiated species or by soaking the material in electrolyte. It would require further development.

The formation and the growth of surface species coming from reaction with  $\text{LiPF}_6$  electrolyte have been subsequently followed by combining analyses of spectra lineshapes and integrated intensities in  ${}^7\text{Li}$  MAS NMR in the case of  $\text{LiNi}_{1/2}\text{Mn}_{1/2}\text{O}_2$  and  $\text{LiFePO}_4$ , two materials amongst promising candidates for positive electrodes for lithium batteries. Concerning the layered nickel manganese oxide, the reaction with electrolyte is extremely fast during the first moments of exposure and slows down for longer exposure times, evolving like a passivation reaction (Fig. 5a). Nevertheless, integrated NMR intensities are not proportional to specific surfaces

of materials. Moreover, the clear overall decrease of the spectra line shapes for longer contact times suggests that the additional species have a weaker interaction with the paramagnetic bulk of active material (Fig. 5b). The slow NMR evolution observed after the initial important increase can be assigned to the stacking of lithium containing species on the top of the initial deposits, instead of further covering of material surface by decomposition products. The formation of discrete deposits instead of an homogenous layer was proven by TEM experiments (Fig. 5c) confirming the ability of NMR experiment to provide topological information about the electrode/electrolyte interphase.  ${}^7\text{Li}$  NMR combined with  ${}^1\text{H}$  NMR<sup>42</sup> and XPS<sup>49,50</sup> experiments on soaked samples displaying initial surface  $\text{Li}_2\text{CO}_3$  showed that these species react with the electrolyte, yielding fluorinated products such as  $\text{Li}_x\text{PF}_y$ ,  $\text{LiF}$ , and  $\text{Li}_x\text{PO}_y\text{F}_z$  for short contact times. Only for a longer

exposure to electrolyte appear organic products coming from the electrolyte solvents decomposition.

Similar  ${}^7\text{Li}$  MAS NMR experiments on  $\text{LiFePO}_4$  samples<sup>51</sup> permitted also to observe the growth of an interphase, the reaction being significantly aggravated in the case of the non-carbon coated material in spite of the smaller grain size and the higher specific surface area of the carbon coated  $\text{LiFePO}_4$ . These results demonstrated the clear influence of the carbon coating as a protection against parasitic reaction with the electrolyte. The interphase grows continuously on olivine particles as no passivation state is reached after one month of contact with the electrolyte contrasting with the behavior of  $\text{LiNi}_{1/2}\text{Mn}_{1/2}\text{O}_2$ . In addition, the integrated intensity of the corresponding  ${}^7\text{Li}$  NMR signal being much lower, it allowed confirming that the two materials display a completely different surface chemistry, not only in terms of chemical nature of the reaction products, as shown in previous XPS and

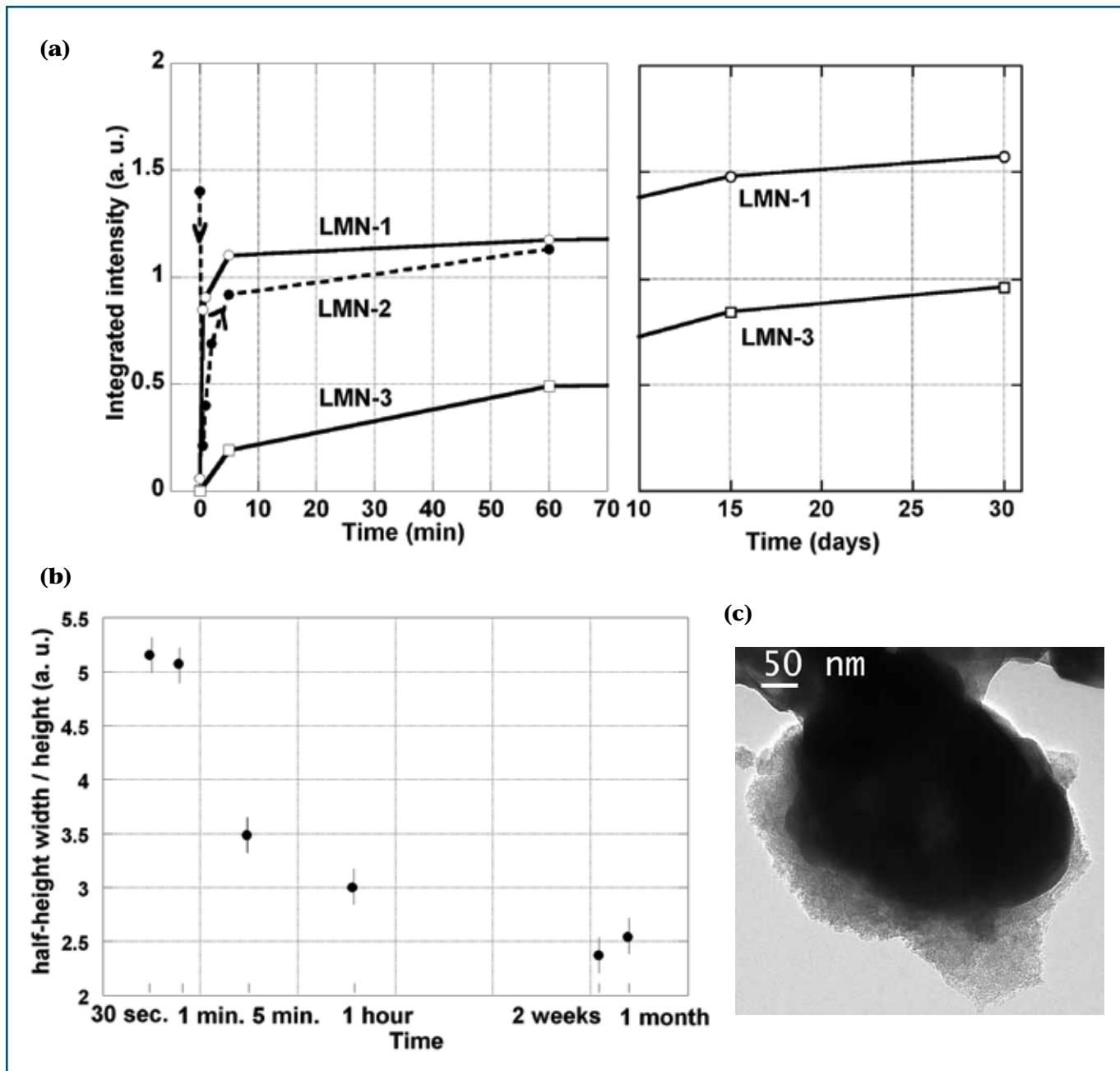


**FIG. 5.** (a) Evolution of the normalized integrated intensities of  ${}^7\text{Li}$  MAS NMR spectra, for different  $\text{LiNi}_{1/2}\text{Mn}_{1/2}\text{O}_2$  samples soaked in  $\text{LiPF}_6$  (EC/DMC 1M) electrolyte for various amounts of time. LMN-1 and LMN-3 were stored in argon and exhibit specific surfaces of  $8\text{ m}^2/\text{g}$  and  $4\text{ m}^2/\text{g}$ , respectively. LMN-2 was stored in air and displays a pristine  $\text{Li}_2\text{CO}_3$  interphase. (b) Half-height width of  ${}^7\text{Li}$  NMR spectra normalized to the height for LMN-1 soaked in  $\text{LiPF}_6$  (EC/DMC 1M) electrolyte for various amounts of time. Estimated errors are reported as vertical bars. (c.) TEM pictures for LMN-1 after 2 weeks of contact with the electrolyte.

FTIR studies,<sup>7,14-18</sup> but also in terms of the surface reactivity towards electrolyte. This result combined with EIS confirmed the very limited role of the interphase on the electrochemical performances of  $\text{LiFePO}_4$  electrodes as opposed to the behavior of most oxides.

These first steps in the characterization of the electrode/electrolyte interface using MAS NMR spectroscopy suggest that a systematic investigation using the NMR characterization should allow some further understanding of the surface layer present on the pristine

positive electrode materials of Li-ion batteries, as well as of the SEI formed during battery operation.  ${}^7\text{Li}$  MAS NMR permitted to follow the evolution of the interphase along the electrochemical cycling of  $\text{LiNi}_{1/2}\text{Mn}_{1/2}\text{O}_2$ .<sup>52,53</sup> The good correlation between the evolution of surface phenomena probed by NMR and bulk properties showed in particular the influence of surface species on the electrochemical behavior. In particular, for air-stored  $\text{LiNi}_{1/2}\text{Mn}_{1/2}\text{O}_2$  the overall electrochemical behavior, which

depends normally on bulk properties, is here strongly driven by the evolution of surface phenomena. On the other hand, for  $\text{LiNi}_{0.5}\text{Mn}_{0.5}\text{O}_2$  protected from air contact, the low amount of surface species and its progressive removal along the continuous decrease of electrochemical performances suggested that the interphase is needed to some extent to protect the electrode from degradation. Semi-quantitative  ${}^7\text{Li}$  NMR experiments performed upon cycling

(continued on next page)

indicated the formation of lithiated interphase species in reduction and their partial removal in oxidation, indicating a dynamic character of the interphase upon cycling. Limitations of the method resides in the small chemical shift range of Li and XPS experiments were required to gather complementary chemical information about the composition of interphase species. In order to achieve further characterization of interphase species,  $^{19}\text{F}$  and  $^{31}\text{P}$  MAS NMR is currently under progress as the wider chemical shift range enables to separated different fluorinated and/or phosphored species such as  $\text{LiF}$  and fluorophosphates ( $\text{LiPF}_6$ ,  $\text{Li}_x\text{PF}_z$ ,  $\text{RPO}_{y/z}$ ).

## Conclusions

$^7\text{Li}$  NMR is a powerful tool to study the surface layer on Li-ion battery electrode materials, especially coupled with techniques giving chemical information such as XPS or FTIR. The use of other nuclei such as  $^{19}\text{F}$  or  $^{31}\text{P}$  as probes of elements contained in the interphase is another straightforward way to gather additional insight on the evolution of the chemical composition of inorganic products of electrolyte decomposition. Concerning the organic part of the interphase, the use of  $^{13}\text{C}$  NMR has proved also to be of great interest to understand the decomposition or reaction pathway of organic solvents even though the need of isotopic enrichment and the sensitivity of  $^{13}\text{C}$  NMR to the presence of paramagnetic centers complicate the detection.

In the case of materials containing transition metals with unpaired electrons, in addition to the chemical composition and quantification, it is possible to extract physical or topological information from electron-nucleus dipolar interaction. Especially in the case of  $^7\text{Li}$  NMR, the advantage of this method lies in the efficient separation of surface signal from paramagnetic bulk signal, allowing the extraction of surface information including intimacy between bulk material and surface phase.

The detection and observation of electrode/electrolyte interphase using NMR technique is now applied to a wide range of cathode and anode materials for lithium-ion batteries and is becoming an efficient characterization tool in this research area. More investigations are necessary however to further explore the possibilities of this new interface characterization technique.

Although the technique is being developed for interface characterisation of Li-ion battery materials, it is clear MAS NMR is applicable to surface or interface characterization in many systems in which surfaces and/or interfaces are of

premier importance such as for instance other electrochemical systems (Ni-MH batteries, supercapacitors, fuel cells) as well as in photovoltaic and catalysis domains.

## About the Authors

**NICOLAS DUPRÉ** received his PhD in 2001 from Université Pierre et Marie Curie-Paris VI working under the direction of Prof. Michel Quarton. Dupré was appointed as a postdoctoral associate at SUNY Stony Brook in 2002, where he worked with Prof. Clare P. Grey. Dupré has been working as a CNRS researcher in the Institut des Matériaux Jean Rouxel (IMN) in Nantes, France since 2005. His current research interests are focused on the study of the behavior of materials for lithium batteries, including electrode/electrolyte interface using solid-state NMR. He may be reached at nicolas.dupre@cnsr-immn.fr.

**MARINE CUISINIER** received her master's degree in 2008 in materials science from the Universities of Rennes 1, France and Turin, Italy in the frame of the MaMaSELF Erasmus Mundus program. She is a now a PhD student in the Institut des Matériaux Jean Rouxel (IMN) in Nantes. Her current focus is on electrode/electrolyte interface studies in lithium batteries. She may be reached at marine.cuisinier@cnsr-immn.fr.

**DOMINIQUE GUYOMARD** obtained his PhD in 1985 in materials science and electrochemistry. From 1990 to 1992, he was a visiting scientist under the supervision of Prof. J. M. Tarascon in Bellcore (U.S.), working on the carbon/spinel manganese oxide Li-ion project. He is now Director of Research at CNRS and the head of the Electrochemical Energy Storage and Transformation Department (EEST) of IMN, with about 30 researchers, gathering the activities on Li batteries, on moderate and high temperature fuels cells, and on calculations and simulations and advanced spectroscopies. His expertise deals with basic and applied solid state electrochemistry, and materials and surface science, applied to the fields of Li-ion & Li metal polymer batteries. More specifically, his research is focused on the conception of new materials for electrode applications, on the use of innovative synthesis techniques, and on the characterization of electrode materials for better understanding of reaction mechanism. He may be reached dominique.guyomard@cnsr-immn.fr.

## References

1. J. M. Tarascon and M. Armand, *Nature*, **414**, 359 (2001).
2. A. S. Arico, P. Bruce, B. Scrosati, J. M. Tarascon, and W. Van Schalkwijk, *Nature Materials*, **4**, 366 (2005).
3. D. Aurbach, B. Markovsky, I. Weissman, E. Levi, and Y. Ein-Eli, *Electrochim. Acta*, **45**, 67 (1999).
4. R. Yazami, *Electrochim. Acta*, **45**, 87 (1999).
5. B. Markovsky, A. Rodkin, Y. S. Cohen, O. Palchik, E. Levi, D. Aurbach, H.-J. Kim, and M. Schmidt, *J. Power Sources*, **119-121**, 504 (2003).
6. L. Larush, E. Zinigrad, Y. Goffer, and D. Aurbach, *Langmuir*, **23**, 12910 (2007).
7. D. Aurbach, B. Markovsky, G. Salitra, E. Markevich, Y. Talyossef, M. Koltypin, L. Nazar, B. Ellis, and D. Kovacheva, *J. Power Sources*, **165**, 491 (2007).
8. D. Aurbach, Y. Talyosef, B. Markovsky, E. Markevich, E. Zinigrad, L. Asraf, J. S. Gnanaraj, and H. J. Kim, *Electrochim. Acta*, **50**, 247 (2004).
9. D. Aurbach, B. Markovsky, A. Rodkin, E. Levi, Y. S. Cohen, H. J. Kim, and M. Schmidt, *Electrochim. Acta*, **47**, 4291 (2002).
10. D. Aurbach, Y. Gofer, and J. Langzam, *J. Electrochem. Soc.*, **136**, 3198 (1989).
11. G. G. Amatucci, C. N. Schmutz, A. Blyr, C. Sigala, A. S. Gozdz, D. Larcher, and J. M. Tarascon, *J. Power Sources*, **69**, 11 (1997).
12. D. Aurbach, M. D. Levi, E. Levi, H. Teller, B. Markovsky, G. Salitra, U. Heider, and L. Heider, *J. Electrochem. Soc.*, **145**, 3024 (1998).
13. E. Ericksson, PhD Thesis, Uppsala University, **2001**.
14. T. Matsushita, K. Dokko, and K. Kanamura, *J. Electrochem. Soc.*, **152**, A2229 (2005).
15. H. Ota, T. Akai, H. Namita, S. Yamaguchi, and M. Nomura, *J. Power Sources*, **119-121**, 567 (2003).
16. B. J. Neudecker, R. A. Zuhr, B. S. Kwak, J. B. Bates, and J. D. Robertson, *J. Electrochem. Soc.*, **145**, 4148 (1998).
17. J. C. Dupin, D. Gonbeau, H. Benqlilou-Moudden, P. Vinatier, and A. Levasseur, *Thin Solid Films*, **384**, 23 (2001).
18. K. Edström, T. Gustafsson, and J. O. Thomas, *Electrochim. Acta*, **50**, 397 (2004).
19. M. Letellier, F. Chevallier, C. Clinard, E. Frackowiak, J. N. Rouzaud, F. Beguin, M. Morcrette, and J. M. Tarascon, *J. Chem. Phys.*, **118**, 6038 (2003).
20. M. Letellier, F. Chevallier, and M. Morcrette, *Carbon*, **45**, 1025 (2007).

21. B. Key, R. Bhattacharyya, M. Morcrette, V. Seznec, J. M. Tarascon, and C. P. Grey, *J. Am. Chem. Soc.*, **131**, 9239 (2009).
22. C. P. Grey and N. Dupré, *Chem. Rev.*, **104**, 4493 (2004).
23. M. C. Smart, B. V. Ratnakumar, S. Surampudi, Y. Wang, X. Zhang, S. G. Greenbaum, A. Hightower, C. C. Ahn, and B. Fultz, *J. Electrochem. Soc.*, **146**, 3963 (1999).
24. Y. Wang, X. Guo, S. Greenbaum, J. Liu, and K. Amine, *Electrochem. Solid-State Lett.*, **4**, A68 (2001).
25. M. C. Tucker, A. Braun, U. Bergmann, H. Wang, P. Glatzel, J. A. Reimer, and E. J. Cairns, *Interfaces, Phenomena and Nanostructures in Lithium Batteries Workshop*, (Eds: A. Landgrebe and R. J. Klinger), *Electrochem. Soc. Proc. Series*, **2001**.
26. Y. Oumellal, N. Delpuech, D. Mazouzi, N. Dupre, J. Gaubicher, P. Moreau, P. Soudan, B. Lestriez, and D. Guyomard, *J. Mat. Chem.*, **21**, 6201 (2011).
27. B. Meyer, N. Leifer, S. Sakamoto, S. Greenbaum, and C. P. Grey, *Electrochem. Solid-State Lett.*, **8**, A145 (2005).
28. A. V. Plakhotnyk, L. Ernst, and R. Schmutzler, *J. Fluorine Chem.*, **126**, 27 (2005).
29. Y. Matsuo, R. Kostecki, and F. McLarnon, *J. Electrochem. Soc.*, **148**, A687 (2001).
30. D. Ostrovskii, F. Ronci, B. Scrosati, and P. Jacobsson, *J. Power Sources*, **103**, 10 (2001).
31. T. Eriksson, A. M. Andersson, C. Gejke, T. Gustafsson, and J. O. Thomas, *Langmuir*, **18**, 3609 (2002).
32. M. Herstedt, M. Stjernedahl, A. Nyten, T. Gustafsson, H. Rensmo, H. Siegbahn, N. Ravet, M. Armand, J. O. Thomas, and K. Edstrom, *Electrochem. Solid-State Lett.*, **6**, A202 (2003).
33. S. W. Song, G. V. Zhuang, and P. N. Ross Jr., *J. Electrochem. Soc.*, **151**, A1162 (2004).
34. N. Leifer, M. C. Smart, G. K. S. Prakash, L. Gonzalez, L. Sanchez, K. A. Smith, P. Bhalla, C. P. Grey, S. And G. Greenbaum, *J. Electrochem. Soc.*, **158**, A471 (2011).
35. I. Nicotera, G. D. McLachlan, G. D. Bennett, I. Plitz, F. Badway, G. G. Amatucci, and S. G. Greenbaum, *Electrochem. Solid-State Lett.*, **10**, A5 (2007).
36. D. Carlier, M. Ménétrier, and C. Delmas, *J. Mater. Chem.*, **11**, 594 (2001).
37. D. Carlier, M. Ménétrier, C. P. Grey, C. Delmas, and G. Ceder, *Phys. Rev. B*, **67**, 174103 (2003).
38. C. Chazel, M. Menetrier, D. Carlier, L. Croguennec, and C. Delmas, *Chem. Mat.*, **19**, 4166 (2007).
39. D. Carlier, M. Menetrier, and C. Delmas, *J. Phys. Chem. C*, **114**, 4749 (2010).
40. W. S. Yoon, Y. Paik, X. Q. Yang, M. Balasubramanian, J. McBreen, and C. P. Grey, *Electrochem. Solid-State Lett.*, **5**, A263 (2002).
41. W. S. Yoon, S. Iannopollo, C. P. Grey, D. Carlier, J. Gorman, J. Reed, and G. Ceder, *Electrochem. Solid-State Lett.*, **7**, A167 (2004).
42. M. Ménétrier, C. Vaysse, L. Croguennec, C. Delmas, C. Jordy, F. Bonhomme, and P. Biensan, *Electrochem. Solid-State Lett.*, **7**, A140 (2004).
43. M. Ménétrier, J. Bains, L. Croguennec, A. Flambard, E. Bekaert, C. Jordy, P. Biensan, and C. Delmas, *J. Solid State Chem.*, **181**, 3303 (2008).
44. L. Croguennec, J. Bains, M. Ménétrier, A. Flambard, E. Bekaert, C. Jordy, Ph. Biensan, and C. Delmas, *J. Electrochem. Soc.*, **156**, A349 (2009).
45. G. H. Kim, J. H. Kim, S. T. Myung, C. S. Yoon, and Y.-K. Sun, *J. Electrochem. Soc.*, **152**, A1707 (2005).
46. S. U. Woo, B. C. Park, C. S. Yoon, S. T. Myung, J. Prakash, and Y. K. Sun, *J. Electrochem. Soc.*, **154**, A649 (2007).
47. S. H. Kang and K. Amine, *J. Power Sources*, **146**, 654 (2005).
48. N. Dupré, J.-F. Martin, D. Guyomard, A. Yamada, and R. Kanno, *J. Mat. Chem.*, **18**, 4266 (2008).
49. N. Dupré, J.-F. Martin, D. Guyomard, A. Yamada, and R. Kanno, *J. Power Sources*, **189**, 557 (2008).
50. N. Dupré, J.-F. Martin, J. Oliveri, P. Soudan, D. Guyomard, A. Yamada, and R. Kanno, *J. Electrochem. Soc.*, **156**, C180 (2009).
51. N. Dupré, J.-F. Martin, J. Degryse, V. Fernandez, P. Soudan, and D. Guyomard, *J. Power Sources*, **195**, 7415 (2010).
52. N. Dupré, J.-F. Martin, J. Oliveri, D. Guyomard, A. Yamada, and R. Kanno, *Electrochem. Comm.*, **10**, 1897 (2008).
53. N. Dupré, J.-F. Martin, J. Oliveri, P. Soudan, D. Guyomard, A. Yamada, and R. Kanno, *J. Power Sources*, **196**, 4791 (2011).

# Why Advertise?

*Interface* is an authoritative yet accessible publication. With new ideas and products emerging at an overwhelmingly rapid pace—your product or service can stand out in a publication that will be read by over 9,000 targeted readers world-wide.

Your advertisement will be read by those hard-to-reach people in the field, actual users and purchasers of computers, both hardware and software; precision instruments, optics, laser technology, and other equipment; materials such as batteries, cells, chemistry, metals, etc.; semiconductor processing equipment; training and travel; outside laboratories; and other publications about computers, materials, and sources.

In today's environment of increasing competition for purchasers of goods and services, few publications can put your message in a more credible, respected editorial environment.

The Electrochemical Society



the society for solid-state and electrochemical science and technology

## ECS • The Electrochemical Society

65 South Main Street, Bldg. D  
Pennington, New Jersey 08534-2839 USA

tel: 609.737.1902 • fax: 609.737.2743  
interface@electrochem.org

[www.electrochem.org](http://www.electrochem.org)